Ocean Dynamics (2016) 66:313–327
DOI 10.1007/s10236-016-0921-7

Strong intrusions of the Northern Mediterranean Current on the eastern Gulf of Lion: insights from in-situ observations and high resolution numerical modelling

Nicolas Barrier[1,2] · **Anne A. Petrenko**[1,2] · **Yann Ourmières**[1,2]

Received: 17 June 2015 / Accepted: 5 January 2016 / Published online: 5 February 2016

Abstract The Northern Mediterranean Current is the return branch of the cyclonic circulation of the northwestern Mediterranean Sea. Because of geostrophic constraints, this warm and oligotrophic current is forced to flow westward along the continental slope of the Gulf of Lion. But, occasionally, it penetrates on the shelf and strongly impacts the local biogeochemistry and in turn the primary production. By combining in situ observations and high-resolution modelling, it is shown that intrusions on the eastern part of the gulf are mainly forced by easterly or northwesterly wind events, through physical mechanisms that are very different in nature. Easterlies induce a piling of water along the Gulf of Lion coast that drives, through geostrophy, an alongshore shelf-intruding current. This intrusive current occurs independently of the stratification and is concomitant with the wind forcing. On the other hand, intrusions due to northwesterlies only occur during stratified conditions and are related to the development of upwellings along the Gulf of Lion coasts. When the upwelling develops, a northwestward alongshore pressure force balances the Coriolis force associated with the onshore flow at depth. When the winds drop, the upwelling relaxes and the onshore flow weakens. Consequently, the Coriolis force no longer counterbalances the pressure force that ultimately dominates the momentum balance, causing the displacement of the Northern Current on the Gulf of Lion shelf approximately 1 day after the wind relaxation. This time lag between the northwesterlies decrease and the intrusions permits to anticipate possible changes in the biogeochemistry of the Gulf of Lion.

Keywords Northern Current · Gulf of Lion · Intrusions · Julio · Upwelling · Cross-shelf exchanges · Wind-setup · Easterlies · Mistral · Tramontane · Northwesterlies

Responsible Editor: Pierre De Mey

✉ Nicolas Barrier
barrier.nicolas@wanadoo.fr

[1] Aix-Marseille Université, CNRS/INSU, IRD, MIO, UM 110, 13288 Marseille, France

[2] Université de Toulon, CNRS/INSU, IRD, MIO, UM 110, 83957 La Garde, France

1 Introduction

Coastal areas are a key environment for the marine ecosystem, since they receive large amounts of nutrients through river outflows that in turn favour phytoplankton activity (Cruzado and Velasquez 1990). They also play a significant role in the global biogeochemical cycles of carbon, nitrogen and phosphorus (Mantoura et al. 1991; Liu et al. 2000). But coastal areas are also subjected to high demographic pressure and consequently to great risks of pollution. In this context, a better understanding of the coastal circulation is critical since it controls the dispersion of anthropogenic and river-discharged pollutants (Huthnance 1995), but also the advection of nutrients and larvae (Largier 2003). This is especially true for the Gulf of Lion, which is a wide and shallow continental shelf in the northwestern Mediterranean Sea (Fig. 1), featuring a heavily urbanised shoreline.

Several forcings influence the coastal circulation in the Gulf of Lion. The Mistral and the Tramontane (hereafter referred to as northwesterlies) are cold and dry continental gustly winds that occur anytime in the year. They are highly constrained by the orography (Rhône river valley for the Mistral, Pyrenees and Massif Central for the Tramontane) and may therefore be associated with strong wind curls

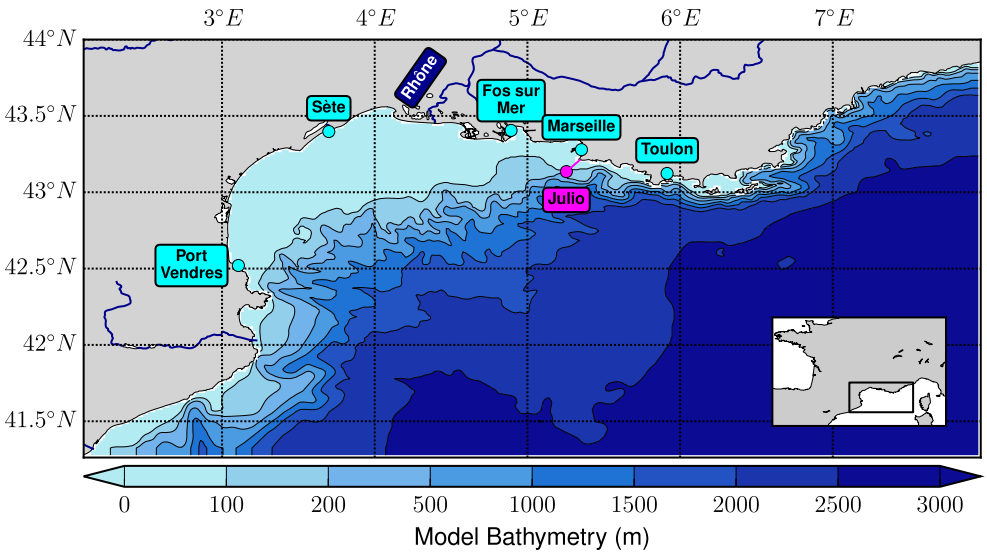

Fig. 1 Bathymetry of the Glazur64 configuration. The locations of the Julio mooring and section are indicated by a *magenta point* and a *magenta line*, respectively

when they reach the gulf. In winter, through cooling and evaporation, they may trigger dense water formation and cascading on the continental shelf (Ulses et al. 2008). While, in summer, they are associated with the development of upwellings (Millot 1979). East-southeast winds (hereafter referred to as easterlies) carry clouds and rain over the Gulf of Lion and are associated with downwellings. They are less frequent than northwesterlies and are especially strong from autumn to spring (Millot 1990). In addition to wind forcing, the Gulf of Lion is subjected to the freshwater inputs of the Rhône River, whose plume can extend over large areas when a strong volume discharge is combined with a shallow thermocline (Fraysse et al. 2014). The associated changes in the density field can impact the shelf circulation (Estournel et al. 2001; Reffray et al. 2004; André et al. 2005).

The coastal circulation in the Gulf of Lion is also strongly influenced by the large-scale ocean circulation of the Mediterranean Sea. The Northern Current, also known as the "Liguro-Provencal Current", is the northern branch of the cyclonic gyre circulation of the northwestern Mediterranean Sea (Millot 1999). It originates before the Ligurian Sea from the merging of the Western and Eastern Corsican Currents (Astraldi et al. 1990). This baroclinic current is, at first order, in geostrophic balance and flows westward along the continental shelf. During winter and certain upwelling conditions, the Northern Current separates the fresh and nutrient-rich coastal waters from the salty and oligotrophic offshore waters. But, as evidenced in observations and numerical modelling, the Northern Current occasionally penetrates over the Gulf of Lion, causing drastic changes in the biogeochemistry and in turn in the primary production on the shelf (Ross et al. 2016).

Intrusions of a slope current on an adjacent shelf have already been evidenced elsewhere in the world ocean, such as the surface intrusions of the Gulf Stream (Oey et al. 1987; Gawarkiewicz et al. 1992) and of the Kuroshio (Chen et al. 1996; Tang et al. 1999; Wu et al. 2005; Caruso et al. 2006). Oey et al. (1987) and Chen et al. (1996) suggest that these intrusions are forced by wind-induced onshore Ekman transport, while Wu et al. (2005) and Caruso et al. (2006) suggest that they are forced by strong wind-stress curls. Other causes are also proposed, such as the meanderings of the main current (Oey et al. 1987) or the abrupt changes in bottom topography (Chen et al. 1996).

The Gulf-Stream and the Kurushio currents are poleward currents that are strongly influenced by the β-effect, contrary to the Northern Current that is more zonally oriented. Other intrusions, more similar to those occurring on the Gulf of Lion, have been evidenced on the northwestern shelf of the Black Sea (Oguz and Besiktepe 1999; Korotaev et al. 2003) or on the Papua Gulf in New Guinea (Wolanski et al. 1995). However, the physical mechanisms of these intrusions are not fully understood yet.

Intrusions of the Northern Current on the eastern part of the Gulf of Lion have been investigated by Gatti et al. (2006) and Gatti (2008), using a combination of in situ observations and numerical modelling. The authors suggest that some intrusions are forced by easterlies, either through

Ekman transport or a shoreward displacement of the Northern Current. They also propose that northwesterlies may favour intrusions through the associated positive wind-stress curl, which would provide a source of vorticity to the Northern Current that may drive intrusions. They also suggest that intrusions on the eastern part of the Gulf of Lion may also occur after the relaxation of upwelling-favourable winds, as shown by Millot and Wald (1980). Using an analytical model combined with numerical simulations, Echevin et al. (2003) assessed the interaction between a coastal current, represented as a baroclinic Kelvin wave, and a shelf break. They suggest that Ekman transport associated with southeasterlies induce a downwelling, which in turn generates a westward coastal current that transports Northern Current waters onto the shelf.

Therefore, although the intrusions of the Northern Current on the eastern part of the Gulf of Lion have been shown to be mainly wind-driven, the associated physical mechanisms remain unclear. Furthermore, the potential influence of the ocean stratification is also not well understood. For instance, Millot and Wald (1980) suggest that intrusions of the Northern Current occur when the ocean is stratified, while Petrenko (2003) has shown that intrusions may be observed independently of stratification.

The aim of the present study is to address these uncertainties and therefore to gain more understanding on the physical mechanisms behind the intrusions of slope currents on continental shelves. Using a combination of ADCP current observations, tide-gauge data and regional high resolution numerical modelling, the physical mechanisms that link the wind forcing and the intrusions on the eastern part of the Gulf of Lion are investigated for the 2012–2013 period. The paper is organised as follows. In Section 2, the observations and numerical model are described. In Section 3, the methodology used in the detection of simulated and observed intrusions is presented. Section 4 is dedicated to the analysis of the physical mechanisms that drive the intrusions. Conclusions and discussions are provided in Section 5.

2 Data description

2.1 Julio mooring

Gatti (2008) has suggested that the Julio[1] site, located on the 100-m isobath at 5.255° E–43.135° N (magenta point in Fig. 1), is a judicious location for the observation of intrusions occurring on the eastern side of the Gulf of Lion. As such, it has been proposed as a site in the framework of the MOOSE[2] observing system (http://www.moose-network.fr/). A bottom-moored ADCP (RDI Ocean Sentinel, 300 kHz) at the Julio site is exploited from 2012 February 12 to 2012 October 23 and from 2013 September 26 to 2013 December 31. It provides measurements of the horizontal currents every 30 min and every 4-m depth between 15 and 92 m.

2.2 Sonel tide-gauge data

Daily tide-gauge observations at Fos sur Mer, Sète and Port Vendres (see locations on Fig. 1) are downloaded from the Sonel website (Sonel stands for "Système d'Observation du Niveau des Eaux Littorales"; website: http://www.sonel.org/). The inverted barometer effect η^{ibc} is computed following Ponte (2006) by:

$$\eta^{ibc} = -\frac{p_a - \overline{p_a}}{\rho_0 g}$$

and is subtracted from the raw daily timeseries. p_a is the atmospheric sea-level pressure and $\overline{p_a}$ its long-term mean (computed on the 1979–2014 period), ρ_0 is the reference density of water (here, 1000 kg m^{-3}) and g is the gravity. The sea-level pressure used here is issued from the ERA-Interim reanalysis of the European Centre for Medium-Range Weather Forecasts (Dee et al. 2011).

2.3 High-resolution numerical modelling

The physical mechanisms that drive the intrusions of the Northern Current on the eastern part of the Gulf of Lion are investigated using the high resolution model simulation of Guihou et al. (2013), which is derived from the Glazur64 configuration of Ourmières et al. (2011). Glazur64 is based on the "Nucleus for European Modelling of the Ocean" modelling framework (NEMO, Madec 2008) and is implemented on a 1/64° regular grid with 130 vertical z-levels, spacing from 1 m near the surface to 30 m near the bottom. Radiative boundary conditions (Cailleau et al. 2008) are used at the eastern and southern parts of the domain, with boundary data, with boundary data prepared from the basin-scale PSY2V4R1 operational configuration provided by MERCATOR-OCEAN (http://www.mercator-ocean.fr). The damping coefficients for the inflows and the outflows are 1 and 10 days, respectively.

[1] Judicious Location for Intrusion Observation.

[2] Mediterranean Ocean Observing System for the Environment.

Surface boundary conditions are provided by the Météo France operational regional model Aladin. This atmospheric model features data assimilation and state-of-the-art atmospheric physics (Fischer et al. 2005). It has a horizontal resolution of around 1/10° (9.5 km) and forcings are provided every 3 h. Such spatiotemporal resolution has been shown to well reproduce specific wind systems, diurnal cycles and sea breeze, hence leading to a valuable improvement of the mesoscale circulation simulated by the ocean model (Schaeffer et al. 2011). The reader interested in the details of the Glazur64 configuration is referred to Guihou et al. (2013).

2.4 Comparison of Glazur64 with the Julio mooring

The time-averaged simulated velocity profiles at the Julio site are compared with the observed ones. The meridional component is fairly well captured by the model simulation, both in term of magnitude and vertical structure (Fig. 2, left panel). However, Glazur64 strongly overestimates the zonal component of the current at the Julio site (Fig. 2, right panel): the simulated zonal velocity is indeed twice as large as the observed one and shows a large weakening at depths, while the observed profile is more homogeneous. This discrepancy is presumably due to a misposition of the simulated Northern Current, which may be too close to the coast hence encroaching on the Julio location. However, this model bias is not critical for the comparison of observed and simulated intrusions. Indeed, more relevant indexes to detect the presence of intrusions will be presented in the following section

3 Detection of Northern Current's intrusions

The intrusions of the Northern Current on the eastern part of the Gulf of Lion have been detected using the Julio ADCP mooring observations as follows. First, the current component that flows perpendicular to the Julio section (magenta line at angle $\theta = 49.4°$ from north in Fig. 1) has been computed using the measured zonal and meridional velocities:

$$U_{jul} = V \cos\theta - U \sin\theta$$

V and U are the meridional and zonal velocities at the Julio mooring. By convention, U_{jul} is counted positive for a northwestward flowing current. Then, U_{jul} has been vertically averaged, hence leading to a half-hourly time-series, on which daily averaging has been performed. Finally, the resulting daily time-series has been standardised: the temporal mean, computed over the overlapping time-period between the observations and model simulation, has been removed and the resulting anomalies have been divided by their standard deviation. The resulting standardized index, which will be referred to as the "observed" Julio index, is shown in Fig. 3 (black line). In the following, we will consider that intrusions occur, in the in situ data, when

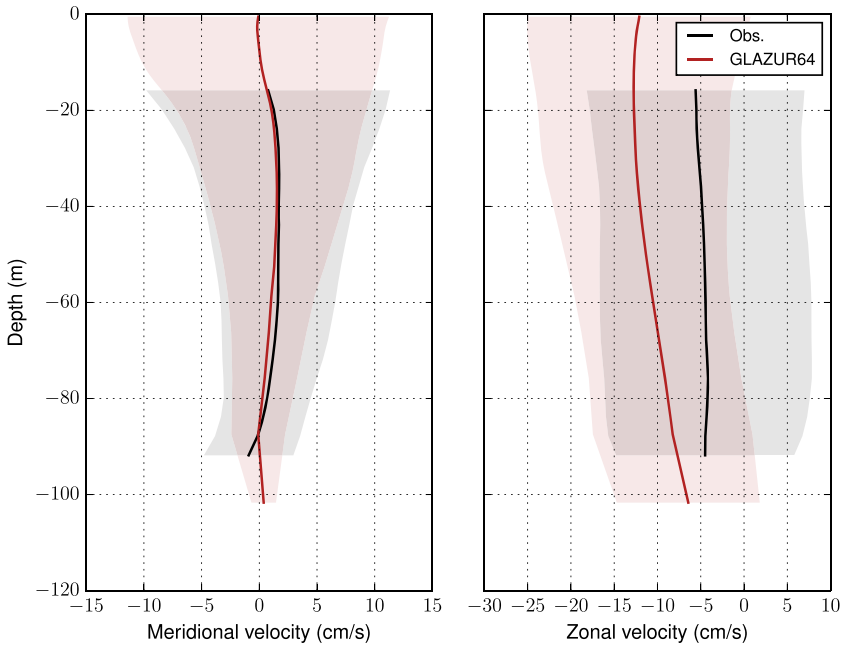

Fig. 2 Time-averaged of the observed (*black*) and simulated (*red*) velocity profiles at the Julio site, computed over the overlapping time period between the observations and model simulation (from February to the end of October 2012, and from October to December 2013). The shadings represent the one-standard deviation envelop

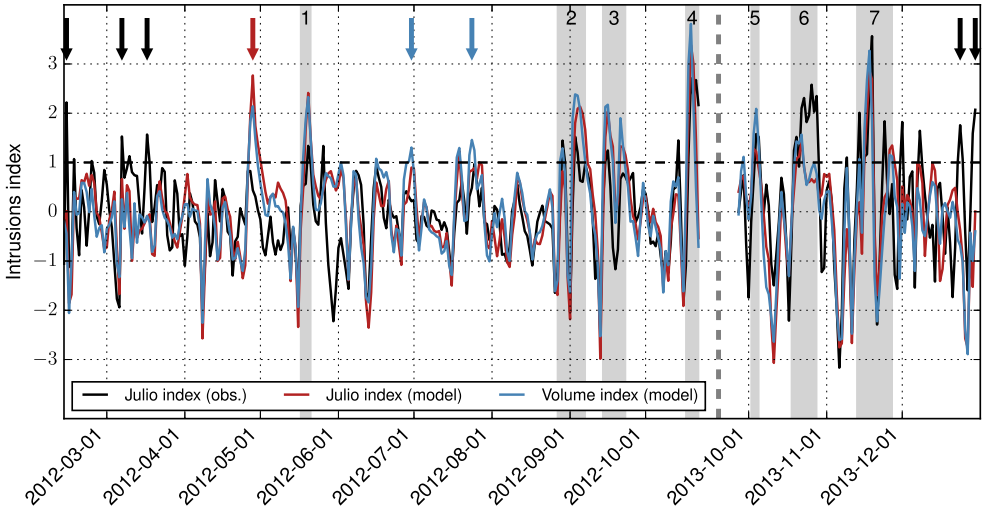

Fig. 3 Observed (*black line*) and simulated (*red* and *blue lines*) standardised intrusion indexes. Only the overlapping time period between the observations and model simulation (from February to the end of October 2012, and from October to December 2013) is shown. *Black arrows* indicate intrusion events that are observed but not simulated, the *red arrow* indicates the simulated intrusion event which is not observed and *blue arrows* highlight simulated intrusions that are captured by the volume index but not by the Julio one. The *vertical dotted line* separates the two time series. The *horizontal dotted line* corresponds to the detection threshold. The *grey shadings* highlight the intrusion events that are investigated in Section 4

the observed Julio index is greater than 1, i.e., when the depth-averaged across-section velocity exceeds its mean by 1 standard deviation.

The same methodology is applied on the Glazur64 model simulation at the grid point the closest to Julio. The simulated standardized Julio index (red line in Fig. 3) shows a correlation of 0.59 with the observed index. This correlation is significant at the 95 % level of confidence, according to a Student t test in which the number of degrees of freedom has been corrected from the 1-day lag autocorrelation of both time series (Bretherton et al. 1999). As shown in Fig. 3, there is a good agreement between the occurrence of the simulated and observed intrusions, in spite of the overestimated zonal velocity simulated at Julio. The model simulation can therefore be considered as robust enough to investigate the physical mechanisms that are responsible for the intrusions.

Nevertheless, there are some examples when the two indexes are out of phase. For example, five intrusion events are observed but are not reproduced in Glazur64 (black arrows on Fig. 3). On 2012 February 14, the observed index has a value of 2.2, while the simulated one has a value of 0.0. On 2012 March 7, the observed index is 1.5 and the simulated one is 0.7, while on 2012 March 17, the observed index is 1.56 and the simulated one is -0.1. On 2012 December 24, the observed Julio index reaches 1.7 and remains above 1 the next day, while the simulated index has a value of -0.4. On 2013 December 29, the observed Julio index reaches 1.6 and increases up to 2.1 the next day, while the simulated Julio index has a value of -1.5. Conversely, one strong intrusion event is simulated on 2012 April 27 by the model but is not observed (red arrow on Fig. 3). At this time, the simulated Julio index reaches 2 and remains above 1 the following 4 days, with a maximum value of 2.8 on 2012 April 28. The observed index also shows an increase but remains below the detection threshold. These discrepancies might be due to an underestimation by the numerical model of the higher levels of instability of the Northern Current during winter or to a misrepresentation of wind forcings by the Aladin model. However, the lack of data observations prevents us from providing robust conclusions. Therefore, we decided to concentrate our efforts on the understanding of the forcing mechanisms of the intrusions that are both observed and simulated.

In order to assess the robustness of the Julio index in the detection of intrusive events, another methodology is added in Glazur64. Daily volume transport across the Julio section is computed by using the "Physical Analysis of the Gridded Ocean" (PAGO) suite of programs (Deshayes et al. 2014).[3] PAGO permits the computation of transport indexes along predefined sections with limited interpolation by connecting two section endpoints as a continuous

[3] See also http://www.whoi.edu/science/PO/pago/.

sequence of grid faces following a great circle pathway. Current velocities along the section do not undergo any interpolation, which allows a better precision on the volume transport calculation. The calculated volume transport is standardised in the same way as the Julio index. This simulated volume index (blue line in Fig. 3) is highly correlated with the simulated Julio index (correlation of 0.92, significant at the 95 % level of confidence), and both simulated indexes detect the same intrusion events. Therefore, the simulated Julio index provides a good indicator of the simulated volume transport across the Julio section, and the comparison between the in situ and simulated Julio indexes provides a good indicator for concomitant intrusion events.

However, we can mention the rare cases of intrusions that are confined very close to the coast. These intrusions are characterized by a simulated volume index that is above 1 and by Julio indexes (observed and simulated) that are less than 1 (blue arrows of Fig. 3). This is for instance the case for the intrusion event that starts on 2012 July 23, during which the simulated volume transport index is above 1 for 3 days, while the simulated Julio index reaches a maximum of 0.9, thus below the detection threshold.

4 Physical mechanisms of the intrusions

In this section, the physical mechanisms associated with the intrusions are investigated. We have focused our attention only on strong intrusion events (grey shadings in Fig. 3, see also Table 1), during which all three intrusion indexes are larger than 1 for at least 1 day, hence corresponding to variations superior to their standard deviations. Moreover, we chose to merge intrusions when only 1 or 2 days separate them. It is the case of intrusions I2 and I3 that both include two intrusions when one looks at the details of Fig. 3. The physical mechanisms associated with these intrusion events are described in the following.

Table 1 List of intrusions that are investigated in Section 4

Number	Start Date	End Date	Wind Forcing
I1	2012-05-18	2012-05-21	NW+E
I2	2012-08-28	2012-09-07	NW
I3	2012-09-15	2012-09-23	NW
I4	2012-10-18	2012-10-22	NW+E
I5	2013-10-03	2013-10-05	E
I6	2013-10-19	2013-10-28	E
I7	2013-11-14	2013-11-27	NW+E

NW stands for northwesterlies and E for easterlies

4.1 Intrusions due to easterlies

Intrusions I5 and I6 occur during easterly wind conditions. In the model simulation, these intrusions are associated with a very strong increase in sea-surface height over the Gulf of Lion, as shown for instance in Fig. 4 for intrusion I6. Such an increase is also evidenced in the Sonel tide-gauge observations: sea-surface height at Fos sur Mer and Sète shows an increase of approximately 20 cm during intrusions I5 and I6 (Fig. 5). This increase is in agreement with the wind setup mechanism proposed by Csanady (1982), which characterizes a balance between the wind-stress and the horizontal pressure gradient force associated with the sea level slope, resulting in a a geostrophic westward alongshore current until 4° E and southwestward west of 4° E.

As discussed in Fraysse et al. (2014), easterlies are also associated with downwelling conditions along the coast. In the model simulation, downwelling indeed occurs, as confirmed by the presence at 20-m depth of diluted freshwater ($S \approx 37.2$) originating from the Rhône river (Fig. 6c), consistently with Fraysse et al. (2014). This freshwater plume is then advected westward past 4° E by the intruding current (Fig. 6d, e). Furthermore, as discussed by Echevin et al. (2003), the downwelling of warm (in summer) and freshwater may also contribute significantly to the westward coastal current.

Figure 7 shows the Hövmoller diagram of the smoothed, daily climatology of the simulated temperature at Julio, which represents well what occurs in the region (data not shown). It is constructed as follows. For each water depth, the daily climatology and the associated FFT coefficients are computed over the 2012–2013 period of the simulation. Next, all the harmonics but the annual and semi-annual ones are set to 0. The smoothed daily climatology is then recovered by a backward transform. As can be inferred from Fig. 7, intrusions I5 and I6 occur in November when the ocean is stratified. However, intrusions induced by easterlies may also occur during unstratified conditions, as for instance between 2012 April 27 and 2012 May 1. As shown in Fig. 3, the simulated Julio and volume indexes are greater than 2, hence, suggesting that a very strong intrusion occurs in the model simulation at this time. This April intrusion shows the same characteristics as intrusions I5 and I6. We can therefore conclude that given the barotropic nature of the mechanism described above, intrusions in response to easterlies occur independently of the stratification.

4.2 Intrusions due to northwesterlies

Intrusions I2 and I3 are induced by strong northwesterly wind bursts on 2012 August 26 and 2012 August 31 for I2 (top panel of Fig. 8), 2012 September 13 and 2012 September 19 for I3. These wind events are followed by intrusions of the Northern Current that reach the Julio location 1 day

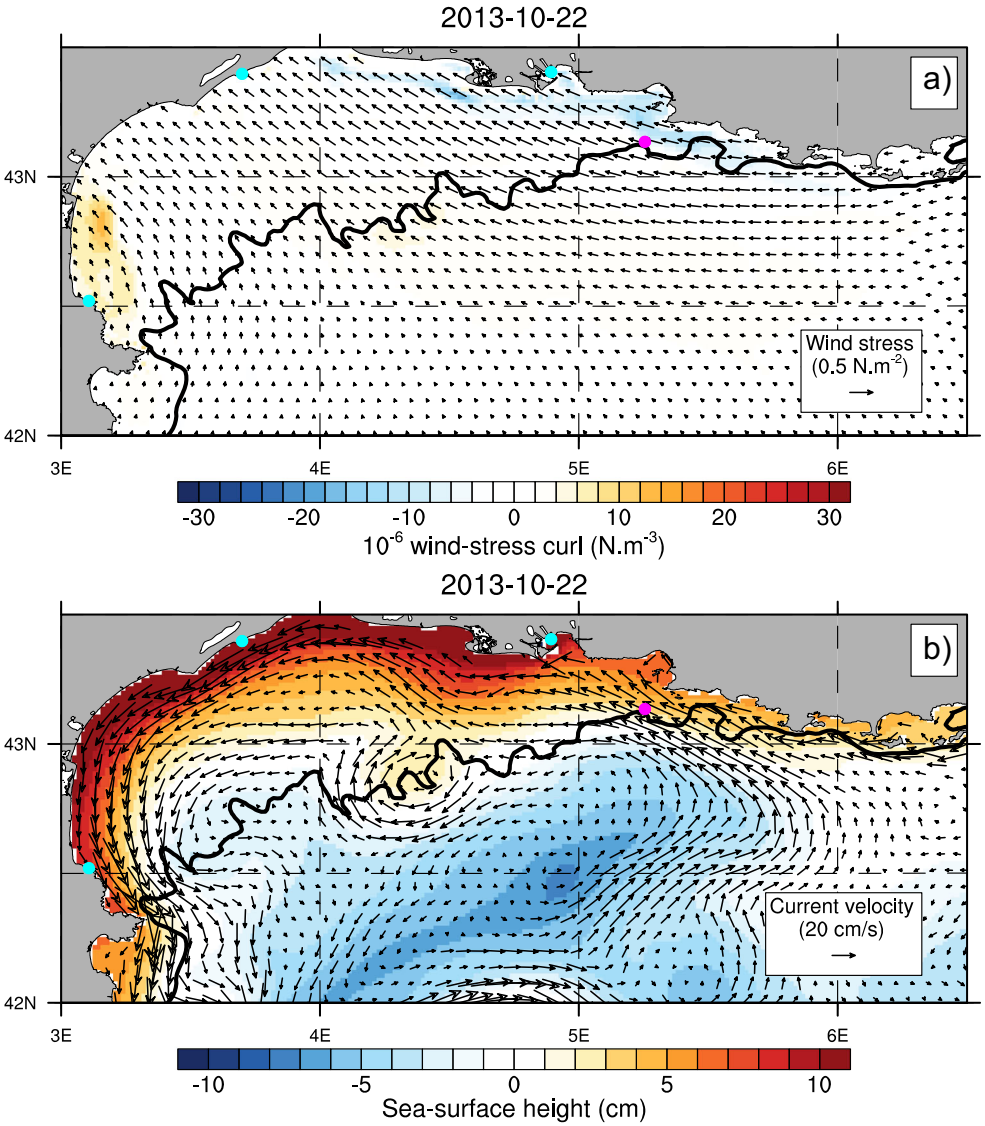

Fig. 4 *Top panel*: simulated wind-stress (*arrows*) and wind-stress curl (*color shadings*) during intrusion I6. *Bottom panel*: simulated sea-surface height (*color shadings*) and 20 m current velocity (*arrows*) during intrusion I6. The locations of the Sonel tide-gauge stations and of the Julio mooring are shown in cyan and magenta, respectively. The 200-m isobath is shown with a *bold black line*

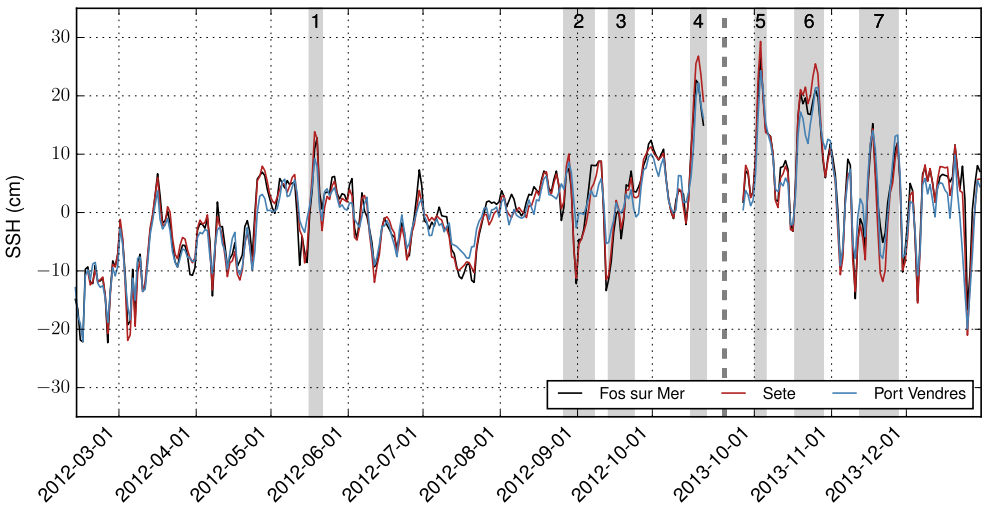

Fig. 5 Daily sea-surface height anomalies from the Sonel dataset corrected from the inverted barometer effect (see Section 2.2 for details). Anomalies have been computed by removing the 2012–2013 mean. The *vertical dotted line* separates the two time series. The *grey shadings* highlight the intrusion events that are investigated in Section 4

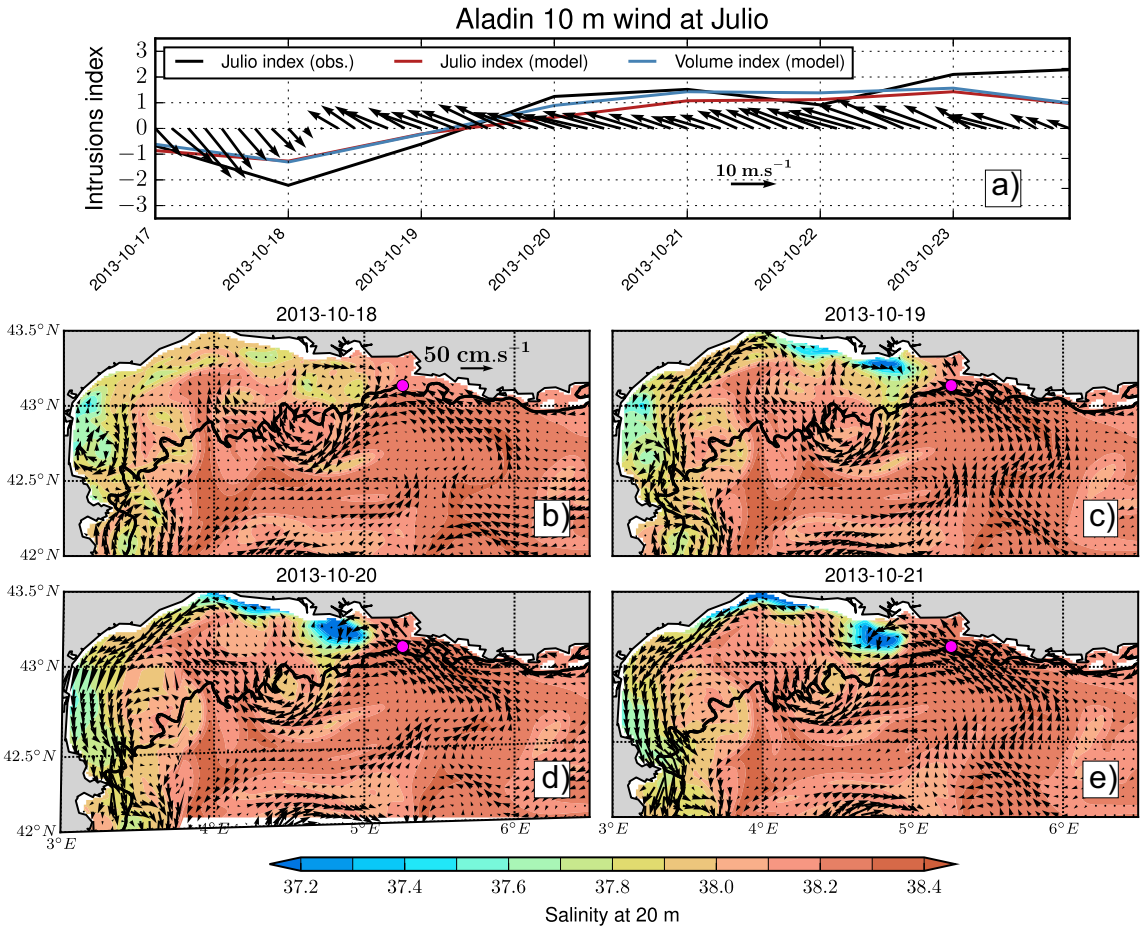

Fig. 6 *Top panel*: Aladin wind at Julio (*arrows*) and intrusion indexes (*lines*). *Bottom panels*: simulated salinity (*color shadings*) and ocean currents (*arrows*) at 20 m during intrusion I6. The 200-m isobath is shown with a *bold black line*

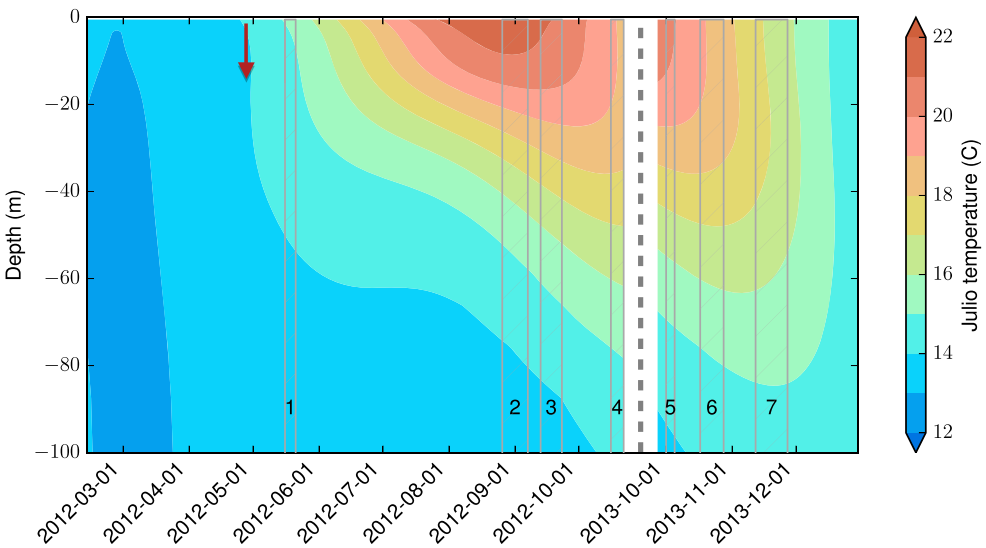

Fig. 7 Hövmoller diagram of the smoothed daily climatology of the simulated temperature at the Julio location (annual and semi-annual harmonics retained, see text for details). The *vertical dotted line* separates the two time series. The *grey hatchings* indicate the intrusion events that are investigated in Section 4

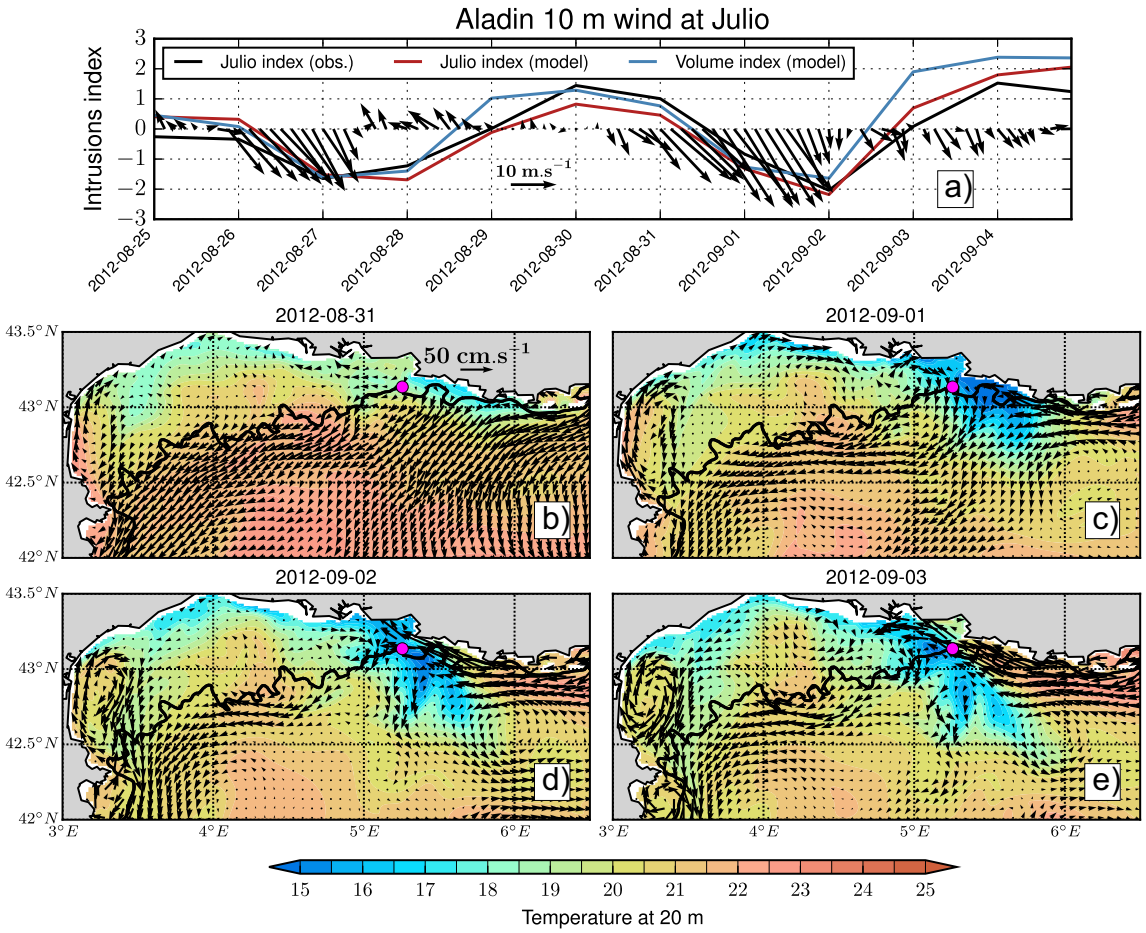

Fig. 8 *Top panel*: Aladin wind at Julio (*arrows*) and intrusion indexes (*lines*). *Bottom panels*: simulated temperature (*color shadings*) and ocean currents (*black arrows*) at 20 m during intrusion I2. The 200-m isobath is shown with a *bold black line*

after the wind relaxation, i.e., on 2012 August 28 and 2012 September 2 for I2, on 2012 September 15 and 2012 September 21 for I3. Indeed, one can observe negative indexes during I2 and I3 concomittant with blowing northwesterlies and positive indexes after their relaxation (top panel of Fig. 8).

Using satellite sea-surface temperature, Millot and Wald (1980) have shown that such wind patterns are favourable to upwellings along the Gulf of Lion coasts and that, when the wind relaxes, the frontal zone between the cold upwelled waters and the warm waters originating from the Northern Current tends to move northwestward and to penetrate over the shelf. As shown in Fig. 8 for intrusion I2, this behaviour is reproduced by the Glazur64 model simulation. When the wind blows, the ocean currents at 20 m beyond the 200 m isobath are southwestward, reflecting the ocean response to wind-stress via Ekman transport (Fig. 8b). Upwellings start developing along the Gulf of Lion coasts and show maximum vertical velocities on the shelf between Marseille and Toulon, collocated with the strongly positive wind-stress curl (data not shown). The upwelling reaches its maximum amplitude on 2012 September 1 (Fig. 8c), when the wind relaxes. The Northern Current reaches the Julio location on 2012 September 2 (Fig. 8d), hence, 1 day after the wind relaxation.

The sea-surface height pattern associated with the intrusions induced by northwesterlies (Fig. 9) is very different from the one associated with the intrusions driven by easterlies (Fig. 4). First, the sea-surface height on the Gulf of Lion coast is not much impacted. This is further confirmed by the observations at the Sonel stations during intrusions I2 and I3, which show a decrease and negative anomalies rather than an increase and positive anomalies associated with easterly-driven intrusions (Fig. 5). Further-

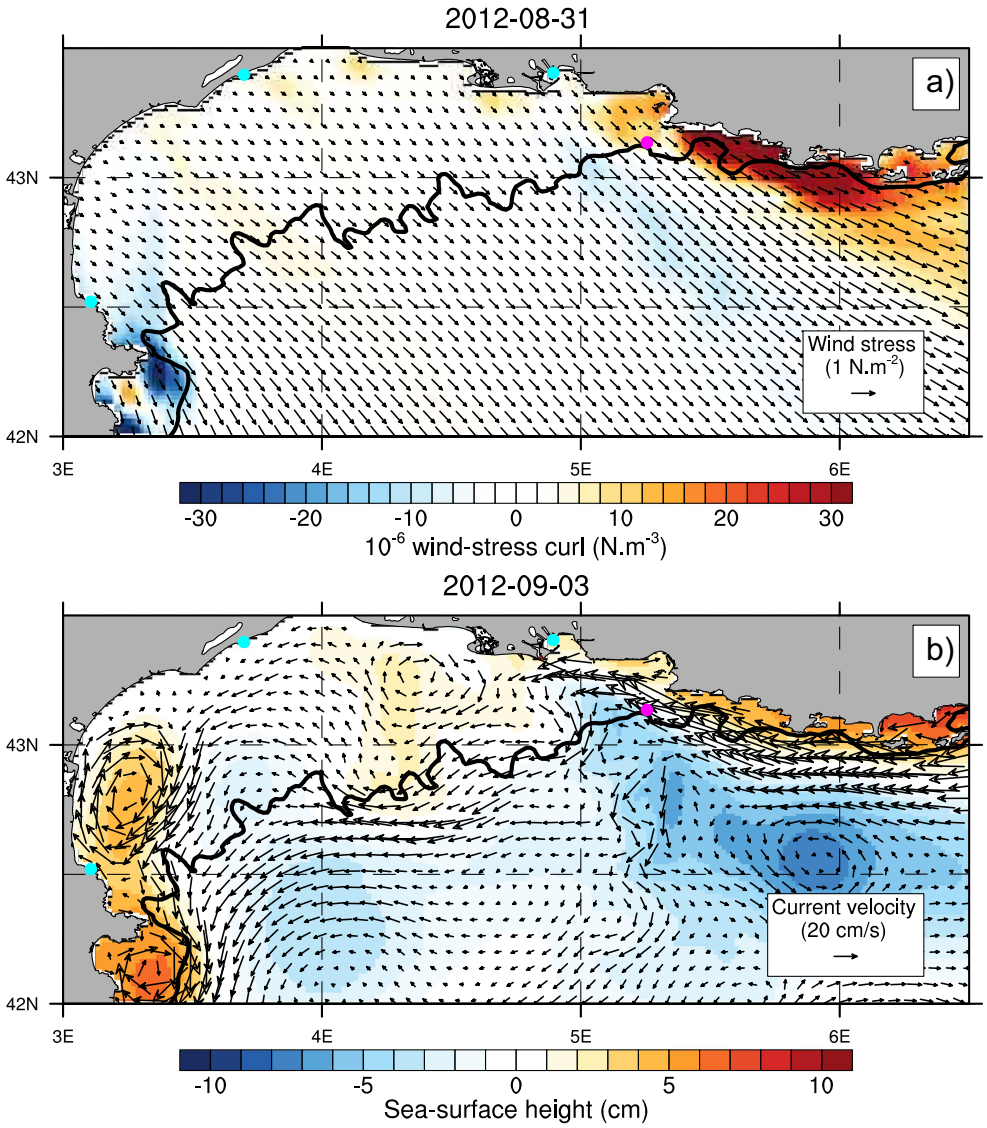

Fig. 9 *Top panel*: simulated wind-stress (*arrows*) and wind-stress curl (*color shadings*) during intrusion I2. *Bottom panel*: simulated sea-surface height (*color shadings*) and 20-m current velocity (*arrows*) during intrusion I2. The locations of the Sonel tide-gauge stations and of the Julio mooring are shown in cyan and magenta, respectively. The 200-m isobath is shown with a *bold black line*

more, one can observe that the sea-surface height pattern on 2012 September 3 (Fig. 9) shows negative values centred at approximately 6° E, 42.5° N, which are tilted northwestward, and positive values on the shelf along the Var coast. The northernmost negative anomalies (near 6° E and 43° N) are collocated and move with the cold temperature pattern of Fig. 8 (Fig. 8c, d, and e). This sea-surface height pattern is associated with positive zonal gradients near 5.25° E and with negative zonal gradients near 5° E. Interestingly, these gradients provide a good indicator of the horizontal pressure gradients at 20 m (data not shown).

This evolution of the Northern Current after northwesterly wind bursts can be related to what happens on the continental shelf off California, as described by Gan and Allen (2002). During northwesterly upwelling favourable winds, eastward pressure gradient force develops west of the Cape Croisette (located south of Marseille, at the north-eastern end of the Julio section, Fig. 1), balancing the nonlinear advective effects, while east of the cape, westward pressure gradient force geostrophically balances the onshore flow at depth. When the northwesterly winds drop, the upwelling relaxes and the Coriolis force no longer counterbalances the

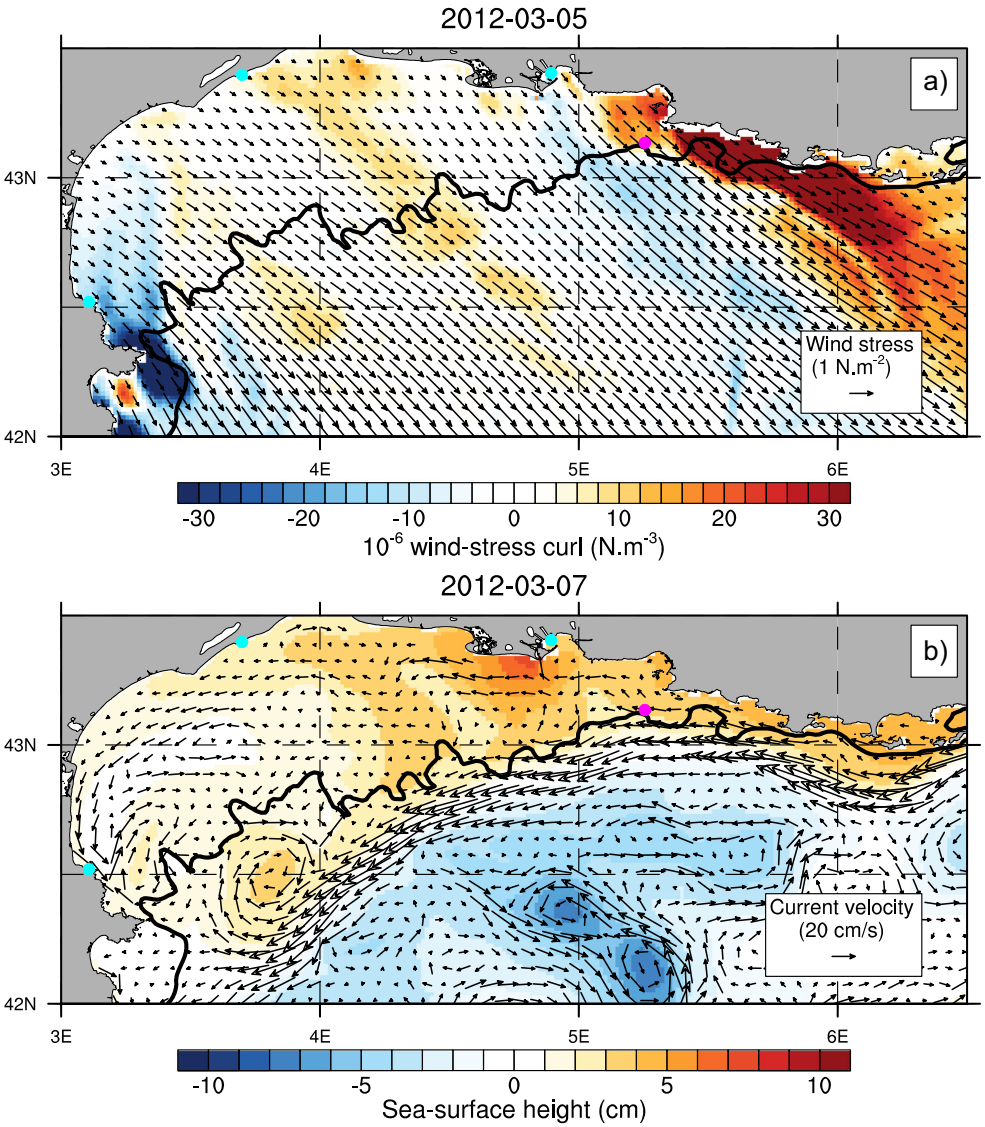

Fig. 10 *Top panel*: simulated wind-stress (*arrows*) and wind-stress curl (*color shadings*) on 2012-03-05. *Bottom panel*: simulated sea-surface height (*color shadings*) and 20-m current velocity (*arrows*) on 2012-03-07. The locations of the Sonel tide-gauge stations and of the Julio mooring are shown in *cyan* and *magenta*, respectively. The 200-m isobath is shown with a *bold black line*

westward pressure force, which ultimately dominates the momentum balance, hence accelerating the current westward. But west of capes, the eastward pressure gradient force is still balanced by the nonlinear advective effects and thus does not contribute to accelerate the current eastward. The net effect is therefore a westward flowing current.

Contrary to easterlies, which may trigger intrusions any time of the year, northwesterlies do not always yield intrusions. For example, in 2012 March 5, the simulated wind-stress is very close to the one simulated on 2012 September 31 (compare Fig. 10 with Fig. 9). But this wind burst is not associated with an upwelling nor with an intrusion on the following days (Fig. 10). The temperature pattern following the wind burst shows colder temperatures on the western Gulf of Lion coasts and rather homogenous temperatures in the open sea (figure not shown). Simulated daily temperature anomalies at Julio, computed by removing the smoothed seasonal cycle shown in Fig. 7, show reduced variance between December and April both at the surface and at 20-m depth (data not shown). This tends to confirm

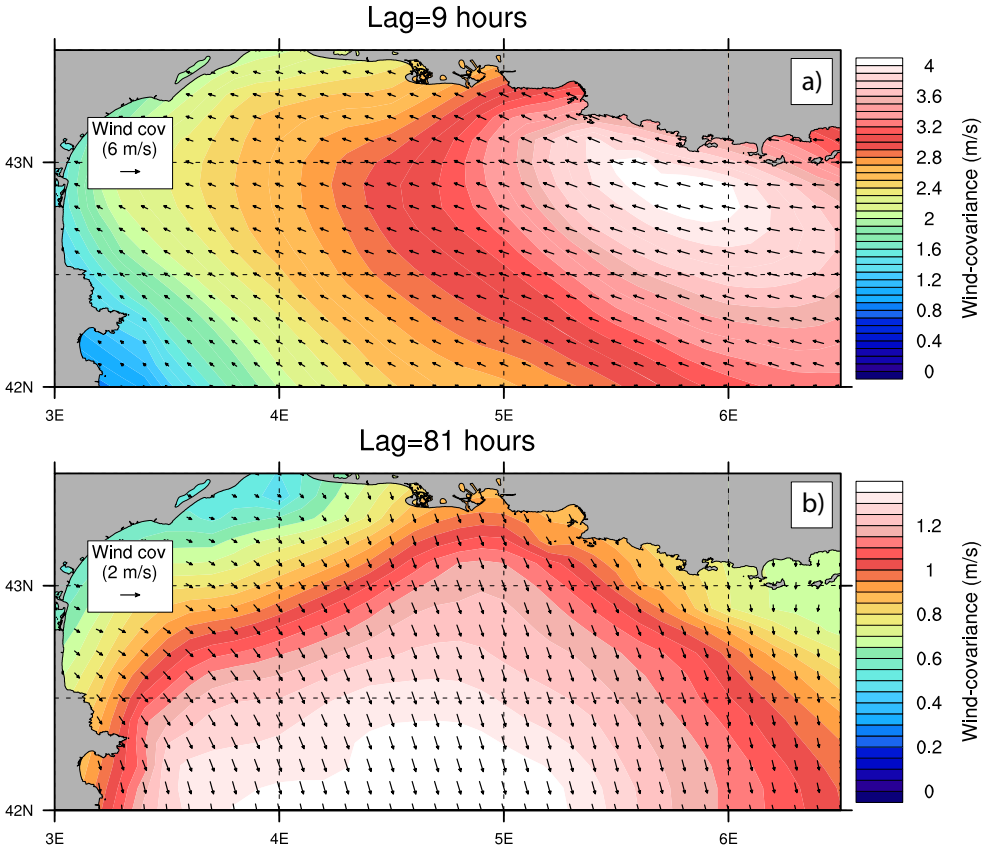

Fig. 11 Covariance at lag 9 h (*top panel*) and 81 h (*bottom panel*) between the 3-hourly standardised Julio index and the Aladin wind anomalies (wind anomalies lead). Note that the *color* and *arrow scales* are different between the two panels

the abscence of upwellings and associated intrusions during the unstratified winter season. A similar behaviour has been evidenced on the North Carolina shelf by Lentz (2001), who suggests that, during unstratified conditions, the wind-driven cross-shelf circulation is weaker because the Ekman depth is greater than the water depth.

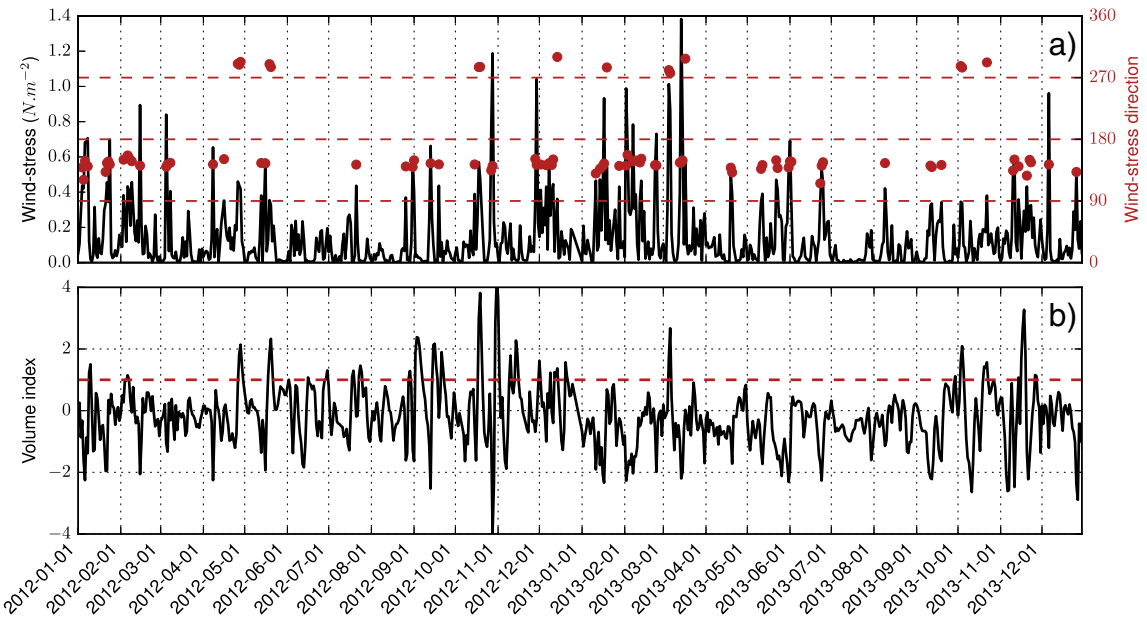

Fig. 12 *Top panel*: Wind-stress amplitude at the Julio location as simulated by the Glazur64 model. *Red dots* indicate the direction of strong wind events (defined as periods when the wind-stress amplitude exceeds the mean by one standard-deviation). Southerlies = 0, Westerlies = 90, Northerlies = 180, Easterlies = 270. *Bottom panel*: simulated volume index over the entire 2012–2013 period. The *dashed line* depicts the intrusion detection criteria

4.3 Combination of both wind patterns

Intrusions I1, I4 and I7 are due to a combination of northwesterlies and easterlies. Intrusion I1 is triggered by a strong northwesterly wind event on 2012 May 16. Following the mechanisms described in Section 4.2, the current starts intruding on the shelf on 2012 May 18. This intrusion is then reinforced by strong easterlies that blow on 2012 May 19 and 2012 May 20, which induce a strong increase in sea-surface height on the western part of the Gulf of Lion and accelerate the intrusive current as discussed in Section 4.1. Similar patterns occur for the other two intrusions. In short, intrusion I4 is triggered by northwesterlies blowing on 2012 October 15 and is reinforced by easterlies blowing between 2012 October 18 and 2012 October 20. Intrusion I7 is triggered by the northwesterlies of 2013 November 14 and reinforced by the easterlies blowing on 2013 November 17 and 2013 November 18.

5 Discussion and conclusions

In this paper, the physical mechanisms associated with the intrusions of the Northern Current on the eastern side of the Gulf of Lion have been investigated using a combination of in situ observations (Julio ADCP mooring and Sonel tide-gauge data) and high resolution numerical modelling. We have shown that easterlies and nortwesterlies are likely to favour such intrusions, but through physical mechanisms that are very different in nature. Easterlies generate intrusions through a wind-setup mechanism and an increase in sea-surface height along the coast, which induces a geostrophic alongshore northwestward coastal current. Because of the barotropic nature of this mechanism, easterlies may trigger intrusions independently of the stratification and thus any time of the year. On the other hand, intrusions in response to northwesterlies principally occur during stratified conditions and are associated with the relaxation of the upwelling that occurs between Marseille and Toulon (Fig. 1). When the upwelling develops, the Coriolis force associated with the onshore flow balances a northwestward pressure gradient force. But when the winds drop and the upwelling relaxes, the Coriolis force weakens and the pressure force dominates the momentum balance. Consequently, the current is advected northwestward and reaches the Julio location approximately 1 day after the wind relaxation. This is very close to the mechanism that takes place in the upwelling system off northern California, as discussed for instance in Gan and Allen (2002).

The difference in the physical mechanisms associated with these two wind patterns may be evidenced using the Julio mooring observations and the Aladin wind fields by using lead-lag covariance analysis. Three-hourly wind-anomalies are first computed by removing the 2012–2013 mean. The lead-lag covariances between these wind-anomalies and the three-hourly Julio index (obtained by averaging the half-hourly across-section velocity and by standardising the resulting time-series) are then computed for each grid point. These covariance maps measure how much the Julio index and the wind anomalies vary together as a function of the time lag between the two series. They have the same units as the wind-anomalies and the visual inspection of the covariance maps shows that the strength of the covariance increases from 0-lag to 9-h lag (wind anomalies lead), at which point it shows a pattern similar to an easterly wind pattern (Fig. 11, top panel). The covariance then decreases in the Gulf of Lion until lag 39 h, where it reaches a minimum. Then, the covariance increases until lag 81 h (approximately 3 days), when it reaches a secondary maximum of weaker amplitude than the first one, looking like a northwesterly-like wind pattern (Fig. 11, bottom panel). This covariance analysis is consistent with the results described in the above, namely a fast response of the Northern Current intrusions to easterlies and a delayed response to northwesterlies.

A remaining question, however, is whether easterlies or northwesterlies are necessary or sufficient conditions for intrusions of the Northern Current on the eastern part of the Gulf of Lion. Figure 12a shows the simulated wind-stress at the Julio location and the orientation of strong wind events (defined as periods when the wind-stress amplitude exceeds its mean by one standard-deviation), while Fig. 12b shows the simulated volume index over the entire 2012–2013 period. One can notice that, as discussed in Section 4.1, strong easterly wind events are always associated with a sharp increase in volume transport across the Julio section and can therefore be considered as sufficient conditions for intrusions. However, as discussed in Section 4.2, northwesterlies are associated with intrusions mainly in summer, when the ocean is stratified (cf. Fig. 7). Hence, northwesterlies are not sufficient conditions for intrusions. But some intrusion events may also occur when the wind forcing is weak, as for instance in November 2012. These events correspond to meanders of the Northern Current encroaching on the shelf, which are presumably due to instabilities of the Northern Current, as discussed in Gatti (2008). Therefore, neither type of wind is a necessary condition, since intrusions can occur in the absence of strong wind forcing.

Nevertheless, the results of the present study are promising since they potentially allow to anticipate cross-shore transports and potential intrusions on the shelf of current-carried plankton or pollution. For instance, Berline et al. (2013) suggest, using the Glazur64 model configuration and a Lagrangian particle tracking software, that jellyfishes are more abundant on the Ligurian Sea coast when the Northern Current is close to the shore. Given the results described in the present study, one can suggest that increased transport

of jellyfish on the Gulf of Lion coasts may be anticipated in the case of northwesterly winds under stratified conditions, since the intrusions occur 1 day after the wind relaxes. However, for the intrusions associated with easterlies, since they occur in phase with the wind forcing, the anticipation of jellyfish stranding is likely to depend on the skill of the weather forecast to predict such wind events. Improving our understanding of the physical processes controlling the environmental conditions of coastal regions has significant socio-economical implications, especially regarding fisheries and marine pollution.

Acknowledgments The authors thank Gilles Rougier and Denis Malengros for their technical assistance with the Julio mooring. The Glazur64 simulations were performed using GENCI-IDRIS resources (Grant 2014011707). The analysis and plots of this paper were performed with both Python and the NCAR Command Language (version 6.2.1, 2011, Boulder, Colorado, UCAR/NCAR/CISL/VETS, doi: 10.5065/D6WD3XH5). The authors also acknowledge Julie Gatti, whose thesis strongly influenced this work.

References

André G, Garreau P, Garnier V, Fraunié P (2005) Modelled variability of the sea surface circulation in the North-western Mediterranean Sea and in the Gulf of Lions. Ocean Dyn 55(3–4):294–308. doi:10.1007/s10236-005-0013-6

Astraldi M, Gasparini G, Manzella G, Hopkins T (1990) Temporal variability of currents in the Eastern Ligurian Sea. J Geophys Res-Oceans 95(C2):1515–1522. doi:10.1029/JC095iC02p01515

Berline L, Zakardjian B, Molcard A, Ourmières Y, Guihou K (2013) Modeling jellyfish Pelagia noctiluca transport and stranding in the Ligurian Sea. Mar Pollut Bull 70(1–2):90–99. doi:10.1016/j.marpolbul.2013.02.016

Bretherton C, Widmann M, Dymnikov V, Wallace J, Blade I (1999) The effective number of spatial degrees of freedom of a time-varying field. J Clim 12(7):1990–2009. doi:10.1175/1520-0442(1999)012<1990:TENOSD>2.0.CO;2

Cailleau S, Fedorenko V, Barnier B, Blayo E, Debreu L (2008) Comparison of different numerical methods used to handle the open boundary of a regional ocean circulation model of the Bay of Biscay. Ocean Model 25(1–2):1–16. doi:10.1016/j.ocemod.2008.05.009

Caruso MJ, Gawarkiewicz GG, Beardsley RC (2006) Interannual variability of the Kuroshio intrusion in the South China Sea. J Oceanogr 62(4):559–575. doi:10.1007/s10872-006-0076-0

Chen HT, Yan XH, Shaw PT, Zheng Q (1996) A numerical simulation of wind stress and topographic effects on the Kuroshio current path near Taiwan. J Phys Oceanogr 26(9):1769–1802. doi:10.1175/1520-0485(1996)026<1769:ANSOWS>2.0.CO;2

Cruzado A, Velasquez Z (1990) Nutrients and phytoplankton in the Gulf of Lions, northwestern Mediterranean. Cont Shelf Res 10(9–11):931–942. doi:10.1016/0278-4343(90)90068-W

Csanady GT (1982) Circulation in the coastal ocean. Springer

Dee DP, Uppala SM, Simmons AJ, Berrisford P, Poli P, Kobayashi S, Andrae U, Balmaseda MA, Balsamo G, Bauer P, Bechtold P, Beljaars ACM, van de Berg L, Bidlot J, Bormann N, Delsol C, Dragani R, Fuentes M, Geer AJ, Haimberger L, Healy SB, Hersbach H, Hlm EV, Isaksen L, Kllberg P, Khler M, Matricardi M, McNally AP, Monge-Sanz BM, Morcrette JJ, Park BK, Peubey C, de Rosnay P, Tavolato C, Thépaut JN, Vitart F (2011) The ERA-Interim reanalysis: configuration and performance of the data assimilation system. Q J R Meteorol Soc 137(656):553–597. doi:10.1002/qj.828

Deshayes J, Curry R, Msadek R (2014) CMIP5 Model Intercomparison of Freshwater Budget and Circulation in the North Atlantic. J Clim 27(9):3298–3317. doi:10.1175/JCLI-D-12-00700.1

Echevin V, Crepon M, Mortier L (2003) Interaction of a coastal current with a gulf: application to the shelf circulation of the Gulf of Lions in the Mediterranean Sea. J Phys Oceanogr 33(1):188–206. doi:10.1175/1520-0485(2003)033<0188:IOACCW>2.0.CO;2

Estournel C, Broche P, Marsaleix P, Devenon JL, Auclair F, Vehil R (2001) The Rhone River Plume in unsteady conditions: numerical and experimental results. Estuar Coast Shelf Sci 53(1):25–38. doi:10.1006/ecss.2000.0685

Fischer C, Montmerle T, Berre L, Auger L, Stefanescu SE (2005) An overview of the variational assimilation in the ALADIN/France numerical weather-prediction system. Q J R Meteorol Soc 131(613):3477–3492. doi:10.1256/qj.05.115

Fraysse M, Pairaud I, Ross ON, Faure VM, Pinazo C (2014) Intrusion of Rhone River diluted water into the Bay of Marseille: Generation processes and impacts on ecosystem functioning. J Geophys Res-Oceans 119(10):6535–6556. doi:10.1002/2014JC010022

Gan J, Allen JS (2002) A modeling study of shelf circulation off northern California in the region of the Coastal Ocean Dynamics Experiment: Response to relaxation of upwelling winds. J Geophys Res-Oceans 107(C9):6–1–6–31. doi:10.1029/2000JC000768

Gatti J (2008) Intrusions du Courant Nord Méditerranéen sur la partie est du plateau continental du Golfe du Lion. PhD thesis, Université Aix-Marseille

Gatti J, Petrenko A, Leredde Y, Devenon J (2006) Modelling the intrusions of the northern current on the eastern part of the gulf of lions continental shelf. Geophys Res Abstr 8:00684

Gawarkiewicz G, Church TM, Luther GW, Ferdelman TG, Caruso M (1992) Large-scale penetration of Gulf Stream water onto the Continental Shelf north of Cape Hatteras. Geophys Res Lett 19(4):373–376. doi:10.1029/92GL00225

Guihou K, Marmain J, Ourmières Y, Molcard A, Zakardjian B, Forget P (2013) A case study of the mesoscale dynamics in the North-Western Mediterranean Sea: a combined data–model approach. Ocean Dyn 63(7):793–808. doi:10.1007/s10236-013-0619-z

Huthnance JM (1995) Circulation, exchange and water masses at the ocean margin: the role of physical processes at the shelf edge. Prog Oceanogr 35(4):353–431. doi:10.1016/0079-6611(95)80003-C

Korotaev G, Oguz T, Nikiforov A, Koblinsky C (2003) Seasonal, interannual, and mesoscale variability of the Black Sea upper layer circulation derived from altimeter data. J Geophys Res-Oceans 108(C4). doi:10.1029/2002JC001508

Largier JL (2003) Considerations in estimating larval dispersal distances from oceanographic data. Ecol Appl 13(1):71–89. doi:10.1890/1051-0761(2003)013[0071:CIELDD]2.0.CO;2

Lentz SJ (2001) The influence of stratification on the wind-driven cross-shelf circulation over the North Carolina Shelf. J Phys Oceanogr 31(9):2749–2760. doi:10.1175/1520-0485(2001)031<2749:TIOSOT>2.0.CO;2

Liu KK, Atkinson L, Chen CTA, Gao S, Hall J, MacDonald RW, McManus LT (2000) Exploring continental margin carbon fluxes on a global scale. Eos, Transactions American Geophysical Union 81(52):641–644. doi:10.1029/EO081i052p00641-01

Madec G, The NEMO team (2008) NEMO ocean engine. Note du Pôle de modélisation, Institut Pierre-Simon Laplace (IPSL), France, No 27, ISSN No 1288-1619

Mantoura RFC, Martin JM, Wollast R et al (1991) Ocean margin processes in global change. Wiley

Millot C (1979) Wind induced upwellings in the Gulf of Lions. Oceanol Acta 2(3):261–274

Millot C (1990) The Gulf of Lions' hydrodynamics. Cont Shelf Res 10(9–11):885–894. doi:10.1016/0278-4343(90)90065-T

Millot C (1999) Circulation in the Western Mediterranean Sea. J Mar Syst 20(1–4):423–442. doi:10.1016/S0924-7963(98)00078-5

Millot C, Wald L (1980) The effect of Mistral wind on the Ligurian current near Provence. Oceanol Acta 3(4):399–402

Oey LY, Atkinson LP, Blanton JO (1987) Shoreward intrusion of upper Gulf Stream water onto the US southeastern continental shelf. J Phys Oceanogr 17(12):2318–2333. doi:10.1175/1520-0485(1987)017<2318:SIOUGS>2.0.CO;2

Oguz T, Besiktepe S (1999) Observations on the Rim Current structure, CIW formation and transport in the western Black Sea. Deep Sea Research Part I: Oceanographic Research Papers 46(10):1733–1753. doi:10.1016/S0967-0637(99)00028-X

Ourmières Y, Zakardjian B, Beranger K, Langlais C (2011) Assessment of a NEMO-based downscaling experiment for the North-Western Mediterranean region: impacts on the Northern Current and comparison with ADCP data and altimetry products. Ocean Model 39(3–4):386–404. doi:10.1016/j.ocemod.2011.06.002

Petrenko A (2003) Variability of circulation features in the gulf of lion NW Mediterranean Sea. Importance of inertial currents. Oceanol Acta 26(4):323–338. doi:10.1016/S0399-1784(03)00038-0

Ponte RM (2006) Low-frequency sea level variability and the inverted barometer effect. J Atmos Ocean Technol 23(4):619–629. doi:10.1175/JTECH1864.1

Reffray G, Fraunié P, Marsaleix P (2004) Secondary flows induced by wind forcing in the Rhône region of freshwater influence. Ocean Dyn 54(2):179–196. doi:10.1007/s10236-003-0079-y

Ross O, Fraysse M, Pinazo C, Pairaud I (2016) Impact of an intrusion by the Northern Current on the biogeochemistry in the eastern Gulf of Lion, NW Mediterranean. Estuarine, Coastal and Shelf Science 170(1–9). doi:10.1016/j.ecss.2015.12.022

Schaeffer A, Garreau P, Molcard A, Fraunie P, Seity Y (2011) Influence of high-resolution wind forcing on hydrodynamic modeling of the Gulf of Lions. Ocean Dyn 61(11):1823–1844. doi:10.1007/s10236-011-0442-3

Tang T, Hsueh Y, Yang Y, Ma J (1999) Continental slope flow northeast of Taiwan. J Phys Oceanogr 29(6):1353–1362. doi:10.1175/1520-0485(1999)029<1353:CSFNOT>2.0.CO;2

Ulses C, Estournel C, Puig P, Durrieu de Madron X, Marsaleix P (2008) Dense shelf water cascading in the northwestern mediterranean during the cold winter 2005: Quantification of the export through the gulf of lion and the catalan margin. Geophys Res Lett 35(7):1–6. doi:10.1029/2008GL033257. l07610

Wolanski E, Norro A, King B (1995) Water circulation in the Gulf of Papua. Cont Shelf Res 15(2):185–212. doi:10.1016/0278-4343(94)E0026-I

Wu CR, Tang T, Lin S (2005) Intra-seasonal variation in the velocity field of the northeastern South China Sea. Cont Shelf Res 25(17):2075–2083. doi:10.1016/j.csr.2005.03.005